

1 **Supplementary Information**

2 **Tracking organic compounds in smoke plumes using infrared satellite-based measurements**

3

4 Julieta F. Juncosa Calahorrano¹, Dylan B. Millet¹, Kelley C. Wells¹, Chengyuan Hu¹, Jared F.
5 Brewer¹, Vivienne H. Payne², Wade Permar³, Lu Hu³, Amy P. Sullivan⁴, I-Ting Ku⁴, Emily V.
6 Fischer⁴, Vanessa Selimovic⁵, Kanako Sekimoto⁶, Aaron Lamplugh⁷, Georgios Gkatzelis⁸, Jessica
7 B. Gilman⁹, Matthew Coggon⁹, Carsten Warneke⁹.

8

9 ¹Department of Soil, Water and Climate, University of Minnesota, Minneapolis, MN 55108,
10 USA.

11 ²Jet Propulsion Laboratory, California Institute of Technology, Pasadena, CA, 91011, USA.

12 ³Department of Chemistry and Biochemistry, University of Montana, Missoula, MT, 59812,
13 USA.

14 ⁴Department of Atmospheric Science, Colorado State University, Fort Collins, CO, 80521, USA.

15 ⁵Department of Chemistry, University of Michigan, Ann Arbor, MI, 48109, USA

16 ⁶Graduate School of Nanobioscience, Yokohama City University, Yokohama, Kanagawa
17 Prefecture, Japan

18 ⁷Colorado Department of Public Health and Environment (CDPHE), Denver, CO, 80246, USA

19 ⁸Institute of Climate and Energy Systems, ICE-3: Troposphere, Forschungszentrum Jülich
20 GmbH, Jülich 52428, Germany

21 ⁹National Oceanic and Atmospheric Administration, Chemical Science Laboratory, Boulder, CO,
22 80305, USA.

23

24

25

26

27

28

29

30

31 **Section S1. High-temperature pyrolysis contribution as derived from ethene:methanol**

32

33 Following the Sekimoto et al. (2018) formulation for ethyne and furan, the ratio R of
34 high-temperature to low-temperature pyrolysis contributions can be estimated as:

35
$$R = \frac{High-T}{Low-T} = \frac{ethene/A}{methanol/B} \quad \text{Eq. S1}$$

36 where A (0.0595 ppb ethene/ppb total VOC) and B (0.0946 ppb methanol/ppb total VOC) are the
37 average emission factors under high- T and low- T conditions.

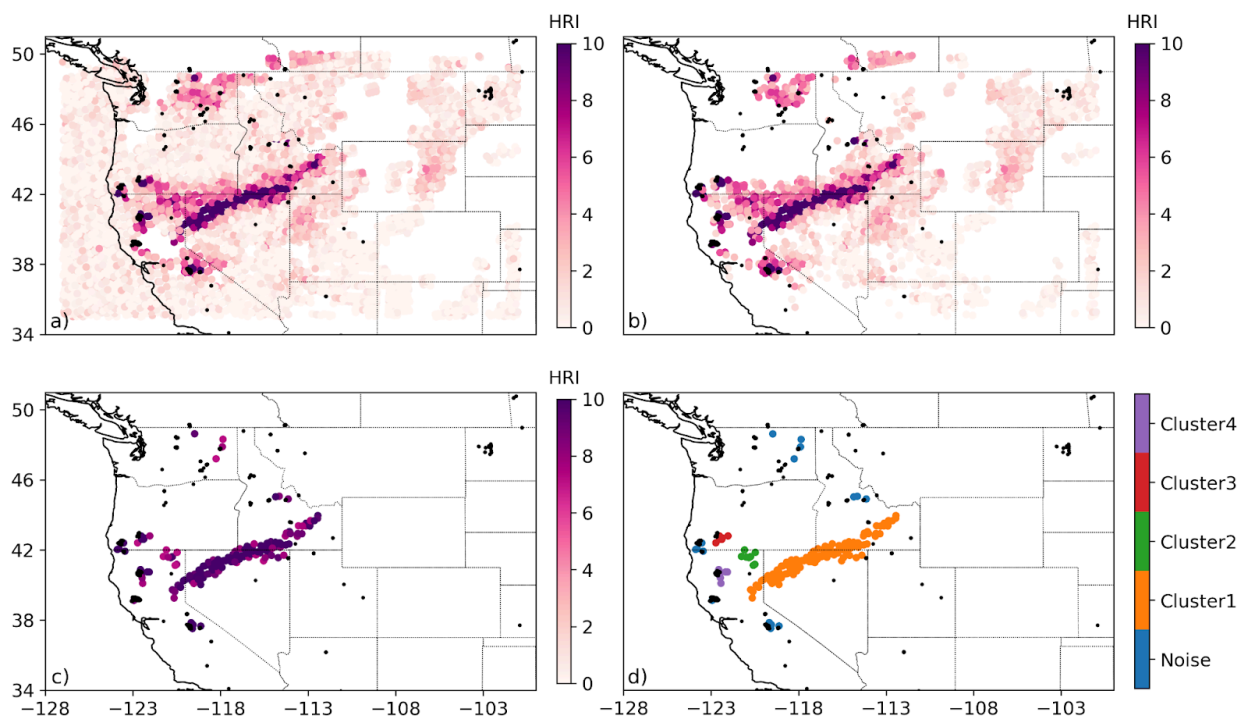
38

39 The fractional contribution F of high- T pyrolysis can then be derived as:

40
$$F = \frac{High-T}{High-T + Low-T} = \frac{R}{1+R} \quad \text{Eq. S2}$$

41

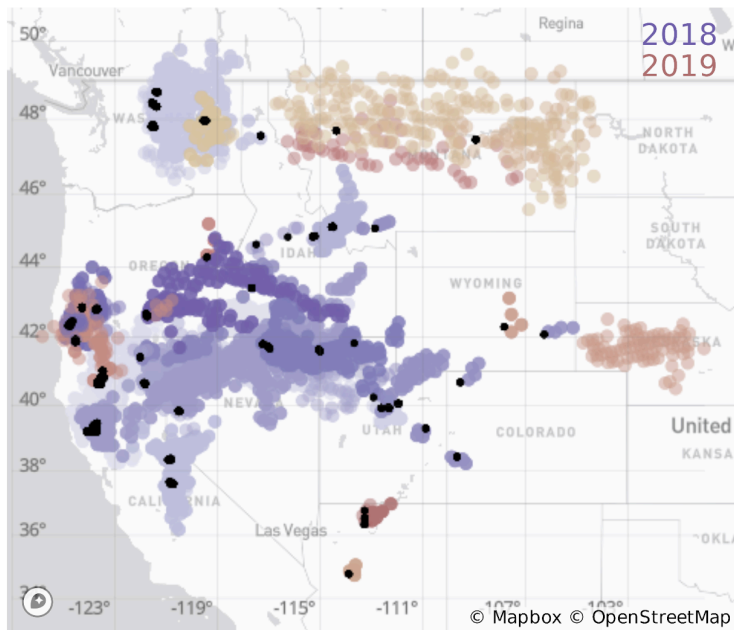
42



43

44 Figure S1. Illustration of smoke selection criteria for August 3, 2018. a) All CrIS ethene
45 observations. b) Smoke-impacted scenes as defined by CrIS CO (>150 ppb at 510 and 680 hPa).
46 c) Dense smoke plumes defined using an additional filter based on CrIS ethene ($HRI > 7$). d)
47 Distinct plume clusters derived using DBSCAN. Black dots show VIIRS daytime fire detections
48 for the same day.

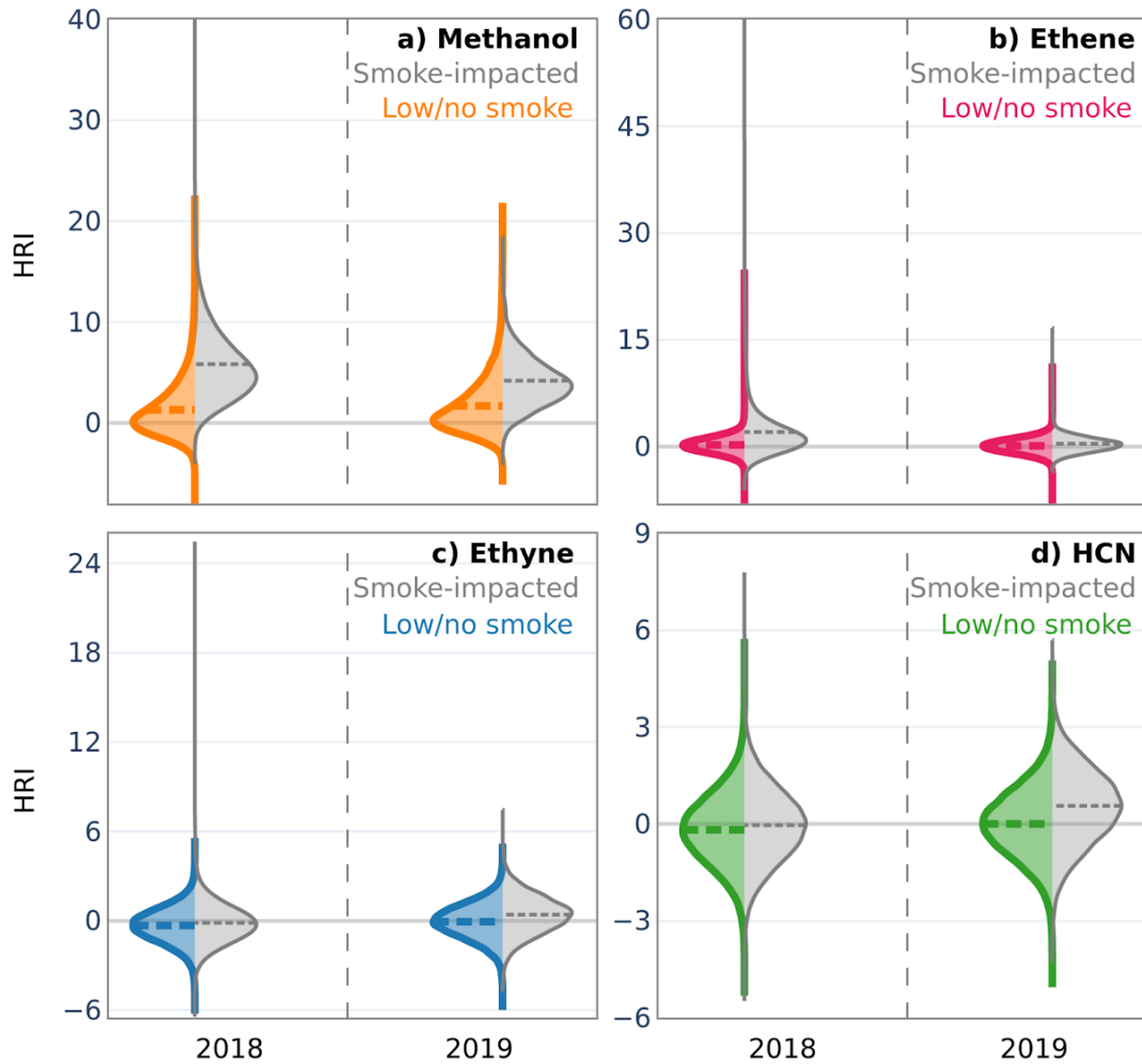
49



50

51 Figure S2. Dense plumes identified using CrIS observations of CO and ethene, grouped via the
52 DBSCAN clustering algorithm. Purple and copper plumes indicate observations from 2018 and
53 2019, respectively. Black dots show the corresponding VIIRS fire detections.

54



55

56 Figure S3. Distribution of VOC spectral signals in low/no-smoke and smoke-impacted scenes

57 over the western U.S. as seen by CrIS during summers 2018 and 2019. Data reflect

58 single-footprint statistics in low/no smoke (color; $N_{2018} = 158,237$; $N_{2019} = 113,044$) and

59 smoke-impacted (grey; $N_{2018} = 108,477$; $N_{2019} = 7,424$) scenes for a) methanol, b) ethene, c)

60 ethyne, and d) HCN. Violin plots show the spread and the probability density of the data using

61 kernel density estimators. The dashed line shows the mean of the distribution in each case.

62 Smoke categories are defined based on CO as described in the text. Figure 2 shows violin plots

63 for the same data aggregated to $0.5^\circ \times 0.5^\circ$ horizontal resolution.

64

65

66 Table S1. Aggregated ($0.5^\circ \times 0.5^\circ$) CrIS HRI statistics in low/no-smoke and smoke-impacted
 67 scenes during the summers of 2018 and 2019

	2018		2019	
	Low/no-smoke mean (\pm std error) [range]	Smoke-impacted mean (\pm std error) [range]	Low/no smoke mean (\pm std error) [range]	Smoke-impacted mean (\pm std error) [range]
Methanol	1.78 (\pm 0.01) [-4.52, 21.97]	5.47 (\pm 0.02) [-2.50, 29.89]	1.84 (\pm 0.01) [-4.44, 16.76]	3.66 (\pm 0.04) [-3.26, 16.36]
Ethene	0.29 (\pm 0.01) [-4.29, 24.24]	1.75 (\pm 0.02) [-3.61, 44.24]	0.05 (\pm 0.01) [-6.30, 7.92]	0.32 (\pm 0.02) [-3.14, 15.41]
Ethyne	-0.35 (\pm 0.01) [-4.77, 3.79]	-0.20 (\pm 0.01) [-4.75, 8.78]	-0.17 (\pm 0.01) [-5.75, 4.35]	0.08 (\pm 0.02) [-4.20, 4.70]
HCN	-0.14 (\pm 0.01) [-4.33, 4.05]	-0.03 (\pm 0.01) [-4.12, 4.62]	0.00 (\pm 0.01) [-4.53, 4.15]	0.28 (\pm 0.02) [-4.53, 4.15]

68

69 Table S2. Single-footprint CrIS HRI statistics in low/no-smoke and smoke-impacted scenes
 70 during the summers of 2018 and 2019

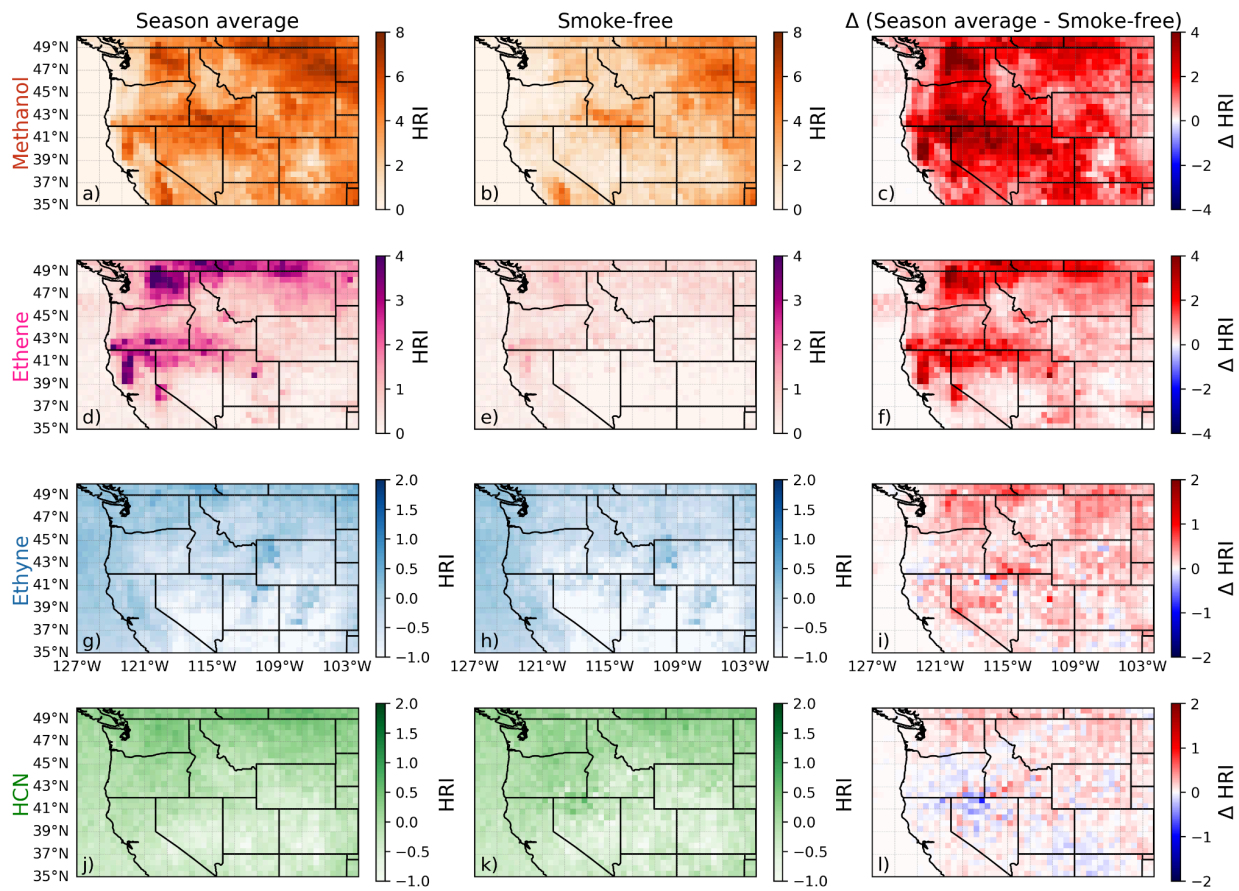
	2018		2019	
	Low/no smoke mean (\pm std error) [range]	Smoke-impacted mean (\pm std error) [range]	Low/no-smoke mean (\pm std error) [range]	Smoke-impacted mean (\pm std error) [range]
Methanol	1.29 (\pm 0.01) [-7.70, 21.97]	5.83 (\pm 0.01) [-2.91, 56.59]	1.68 (\pm 0.01) [-5.58, 21.29]	4.19 (\pm 0.03) [-3.26, 17.62]
Ethene	0.24 (\pm 0.01) [-7.71, 24.24]	2.06 (\pm 0.01) [-3.61, 124.39]	0.09 (\pm 0.01) [-8.79, 11.28]	0.42 (\pm 0.02) [-3.14, 16.28]
Ethyne	-0.31 (\pm 0.01) [-6.01, 5.34]	-0.13 (\pm 0.01) [-5.82, 24.84]	-0.05 (\pm 0.01) [-5.75, 4.94]	0.42 (\pm 0.02) [-4.26, 6.99]
HCN	-0.18 (\pm 0.01) [-5.10, 5.53]	-0.04 (\pm 0.01) [-5.23, 7.55]	0.00 (\pm 0.01) [-4.84, 4.85]	0.56 (\pm 0.01) [-4.84, 4.85]

71

72

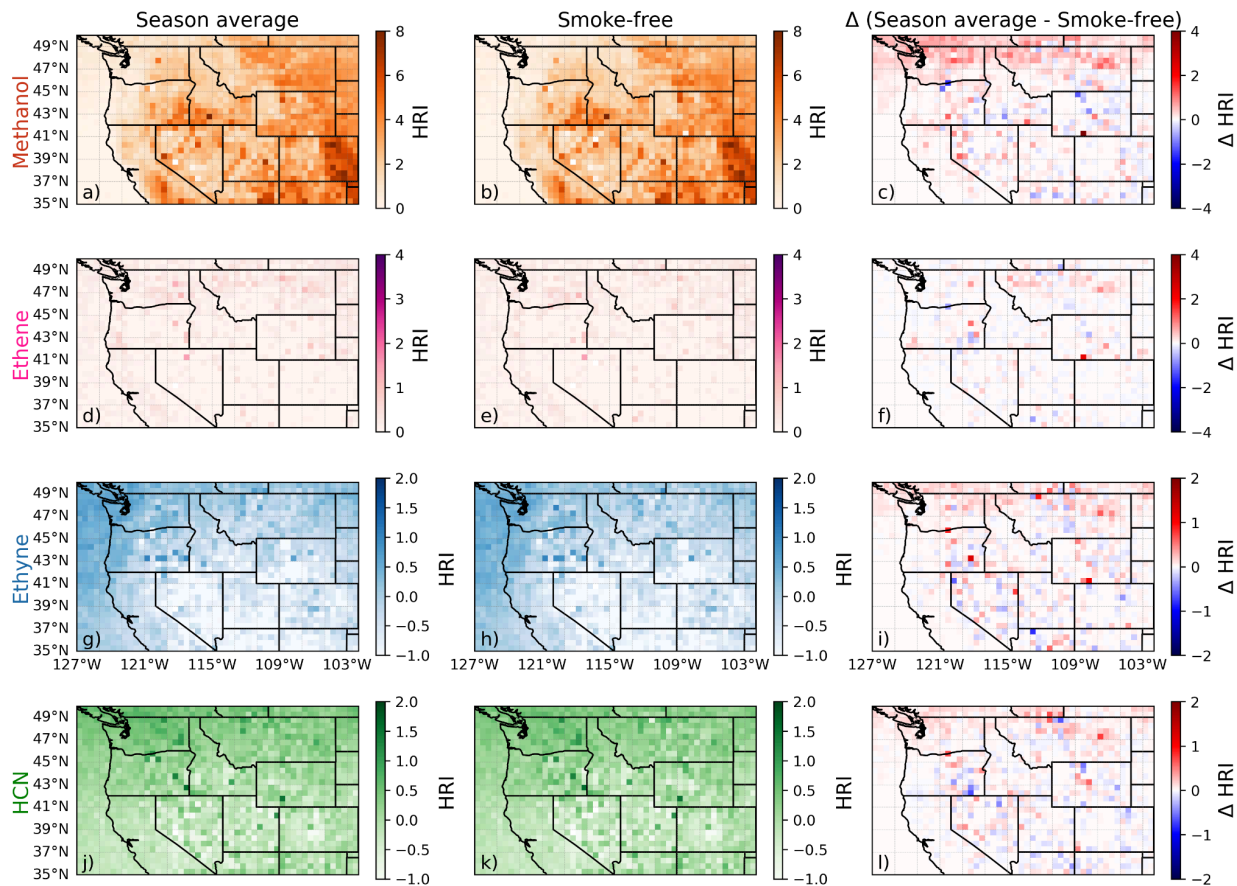
73

74



76

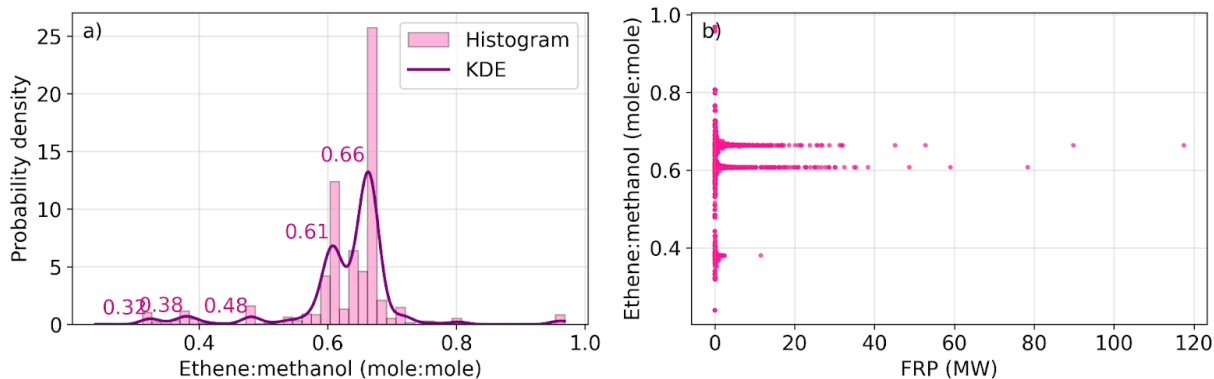
77 Figure S4. Spatial distribution of methanol, ethene, ethyne, and HCN spectral signals (HRIs) as
 78 measured by CrIS from July 24, 2018 - September 13, 2018. The left column shows the mean
 79 measured signal across the entire period, the middle column shows the mean for low/no-smoke
 80 periods, and the right column shows the difference. Data are plotted on a $0.5^\circ \times 0.5^\circ$ grid and
 81 span the WE-CAN campaign timeframe.



82

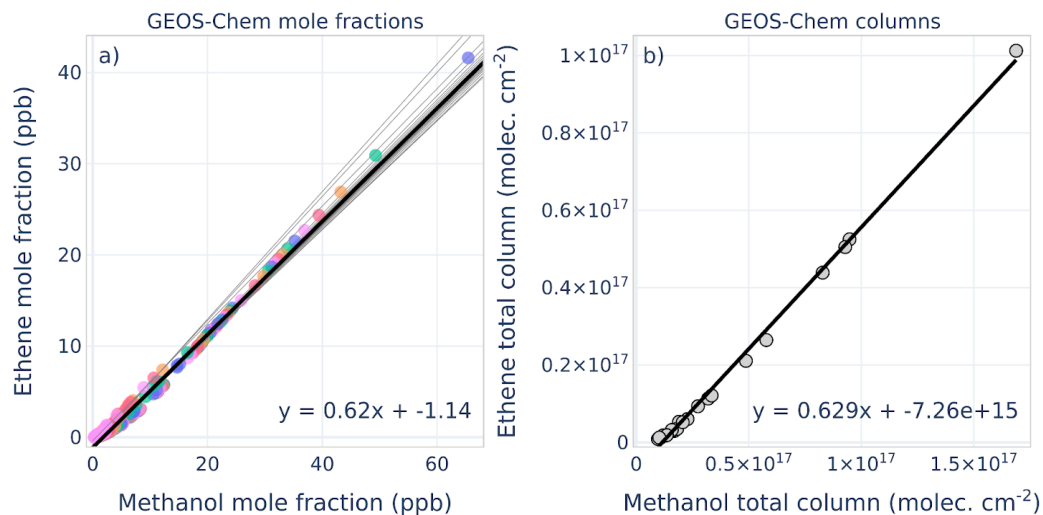
83 Figure S5. Spatial distribution of methanol, ethene, ethyne, and HCN spectral signals (HRIs) as
 84 measured by CrIS from July 26, 2019 - September 6, 2019. The left column shows the mean
 85 measured signal across the entire period, the middle column shows the mean for low/no-smoke
 86 periods, and the right column shows the difference. Data are plotted on a $0.5^\circ \times 0.5^\circ$ grid and
 87 span the FIREX-AQ campaign timeframe.

88



89

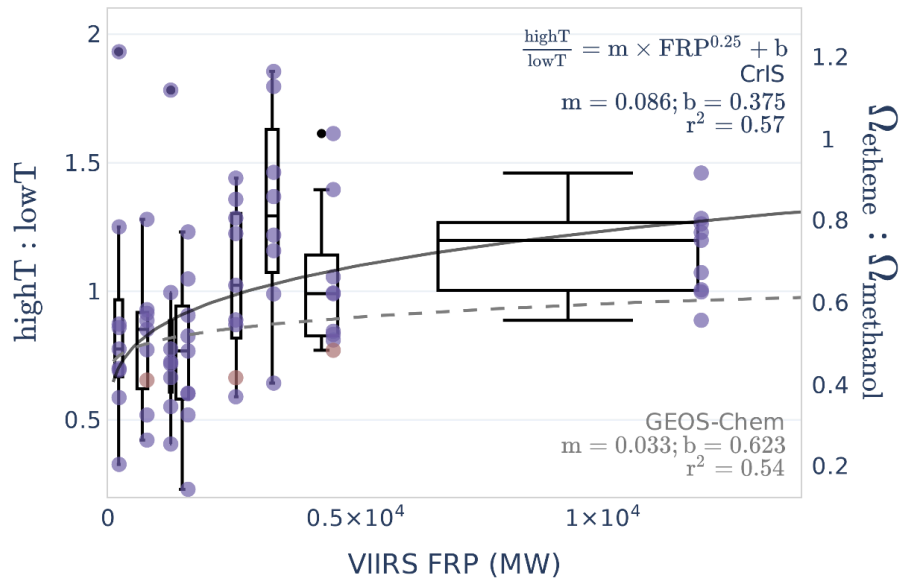
90 Figure S6. a) GFAS ethene:methanol emission ratio distribution for fires during 2018 and 2019
91 over the western U.S. The solid line shows the associated probability density based on kernel
92 density estimation (KDE). b) The same data plotted as a function of GFAS FRP (MW).



93

94 Figure S7. Pyrogenic ethene:methanol ratios are similar when computed using a) in-plume mole
95 fraction and b) total column amounts. Data plotted are from the GEOS-Chem model for the Pole
96 Creek Fire plume. Panel a) shows mole fraction regressions by pressure level from the surface to
97 ~500 hPa (light grey lines) along with the regression across all pressure levels (black line). Panel
98 b) shows a regression for total column values (surface to ~0.1 hPa). In both cases, the derived
99 slopes are close to the molar ethene:methanol emission ratio used in the model for this fire
100 (0.61).

101



102

103 S8. High-T:low-T pyrolysis ratio for each of these fire plumes (estimated from the CrIS
 104 ethene:methanol ratios as described in-text) as a function of VIIRS fire radiative power (FRP).
 105 Right axis shows the CrIS ethene:methanol ratios. Boxplots encompass the interquartile range
 106 (IQR) for each data bin; whiskers span datapoints within $1.5 \times \text{IQR}$ of the first and third quantiles.
 107 Boxplots are positioned at the bin-median FRPs with widths indicating the corresponding
 108 standard deviations. Regression coefficients inset reflect a fourth-root power-law relationship
 109 and are calculated using the median high-T:low-T ratio and FRP for each bin.